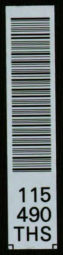

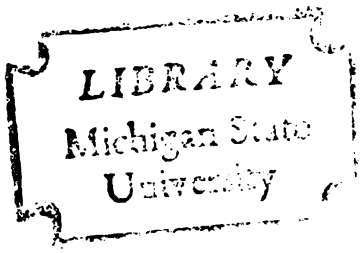

This is to certify that the

thesis entitled

THERMALLY ACTIVATED PROCESS OF DEFORMATION IN FCC SPINODAL MODULATED STRUCTURE

presented by

Tong-Chang Lee

has been accepted towards fulfillment
of the requirements for

M. S. degree in Materials Science

Major professor

Date Feb. 23, 1982

THERMALLY ACTIVATED PROCESS OF DEFORMATION IN FCC SPINODALLY MODULATED STRUCTURE

By

Tong-Chang Lee

A THESIS

Submitted to
Michigan State University
in partial fulfillment of the requirements
for the degree of

MASTER OF SCIENCE

Department of Metallurgy, Mechanics
and Materials Science

1982

ABSTRACT

THERMALLY ACTIVATED PROCESS OF DEFORMATION

IN FCC SPINODALLY MODULATED STRUCTURE

By

Tong- Chang Lee

The mechanism of the thermally activated process of dislocation motion and the temperature dependence of age-hardening in FCC spinodal alloys are discussed theoretically. Numerical calculation has been conducted to evaluate dislocation shapes, activation volume and activation energy associated with the thermal activation process in a two-dimensional periodic field of coherency internal stress. It is found that a double-kink which is similar to that in the Peierls field is formed in the two-dimensional field. From our calculated values of the activation energy and the activation volume of the double-kink formation, it is concluded that the thermal activation process of deformation is very difficult to take place. This explains the experimental observation of the temperature independence of the age-hardening in spinodal alloys. Comparison with the case of one-dimensional periodic field is also presented.

ACKNOWLEDGEMENTS

The author would like to express his deepest appreciation and gratitude to his major advisor Dr. Masaharu Kato for his advice and guidence in both areas of research work and writing of this thesis.

TABLE OF CONTENTS

TABLE OF CONTENTS -- continued

TABLE OF CONTENTS -- continued

LIST OF FIGURES

1 INTRODUCTION

It is generally believed that the age-hardening, i.e., the increase in yield stress during the aging, in spinodal alloys is caused by the coherency internal stress field due to the composition modulation [1 - 4]. According to the experimental studies [5, 6], the age-hardening phenomenon in spinodal alloys is essentially independent of temperature and strain-rate. This fact implies that the thermally activated process of deformation is very difficult to take place in such a system. In the present study, the main emphasis is placed on the theoretical discussion of the mechanism and possibility of the thermally activated deformation process in spinodal alloys in terms of the interaction between a dislocation and the coherent internal stress and the applied stress.

In this chapter, prior art and rationale associated with the present study will be discussed to make our standing point clear.

1.1 Spinodal Decomposition

Let us consider a binary alloy system in which the Helmholtz free energy, F, varies with composition at a temperature T_0 as shown in Figure 1(a). There are two inflection points, C_{s1} and C_{s2}, defined by

$$(\partial^2 F/\partial C^2)_{T,V} = F'' = 0 \ , \qquad (1)$$

where C is the atomic fraction of the secondary component and V is

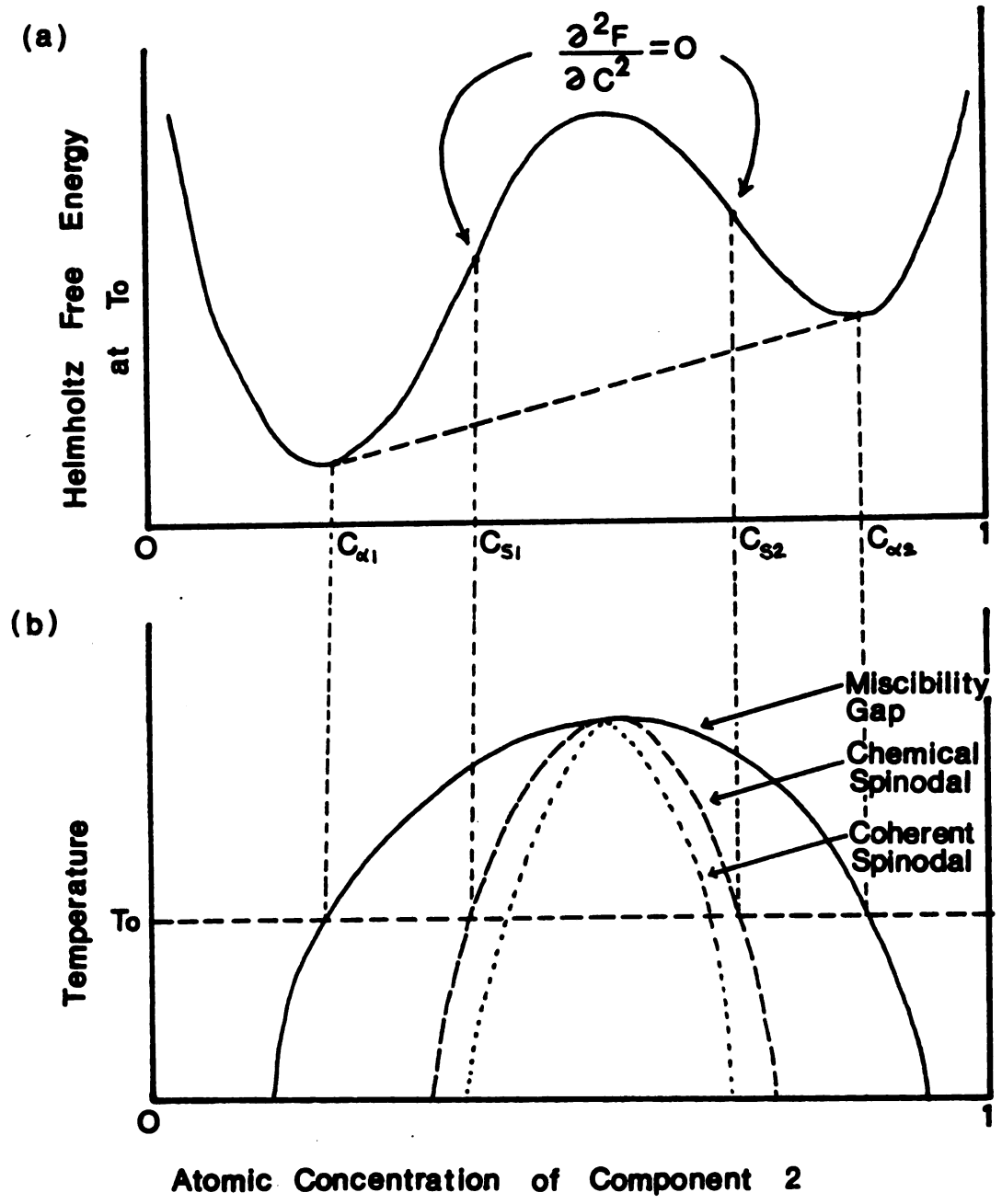

Figure 1 (a) The free energy vs. composition curve at temperature T_o. (b) Binary alloy phase diagram with miscibility gap, chemical spinodal and coherent spinodal.

the volume of the material. $C_{\alpha 1}$ and $C_{\alpha 2}$, on the other hand, are points of common tangency to this curve and they define the composition of the coexisting phases at T_0. The locus of points satisfying equation (1) for different temperatures is called the spinodal (chemical spinodal) and is shown by the dashed curve in Figure 1(b). The solid line in the same figure, the miscibility gap, is the locus of points $C_{\alpha 1}$ and $C_{\alpha 2}$ for different temperatures. For a homogeneous phase with a concentration outside the spinodal at temperature T_0, F" is positive, thus, small fluctuation in composition raises the free energy (except those composition changes are large enough). Thus, this phase is a metastable phase. For a homogeneous phase with a concentration inside the spinodal, F" is negative, thus, this phase is an unstable phase because small fluctuation in concentration always lowers the free energy. Such fluctuation should spontaneously be enhanced until the lowest free energy is achieved, which is a two-phase mixture given by the common tangent. Therefore, the spinodal line can be defined as the boundary between unstable and metastable phases.

The first observation of spinodal decomposition was done in early 1940's. At that time, Bradley [7] reported to have observed sidebands around the sharp Bragg spots of the diffraction pattern from a Cu-Ni-Fe alloy that had been quenched and then annealed inside the miscibility gap. Further observations on the same alloy were made by Daniel and Lipson [8, 9], and concluded that the sidebands could be explained by a periodic modulation of composition in the <100> directions. From the spacing of the sidebands they were able to determine the wavelength of the modulation, which was of the order of 100 Å.

The first explanation of the periodicity was given by Hillert

[10, 11]. Since there is no thermodynamic barrier inside the spinodal, the decomposition is determined solely by diffusion. Hillert derived a flux equation for one-dimensional diffusion on a discrete lattice. This equation differed from the usual classical diffusion equation by including a term that allowed for the effect of the driving force of the interfacial energy between adjacent atomic planes that differed in composition. Hillert solved this equation numerically and found that inside the spinodal it yielded a periodic variation of composition with distance. Furthermore, the wavelengh of the modulation was of the same order as that observed in the Cu-Ni-Fe alloy [12].

A more convenient approach was introduced by Cahn [13, 14] by adding an additional term to equation (1) for the effect of the coherency strains, i.e.,

$$F'' + 2\eta^2 Y = 0 \ , \tag{2}$$

where η is defined by $\partial \ln a / \partial C$ with a as the lattice parameter and C as the concentration of the secondary element, and Y, for the case of the <100> modulation, can be expressed in terms of the elastic constants C_{ij} as

$$Y = \frac{(C_{11} - C_{12})(C_{11} + 2C_{12})}{C_{11}} \ . \tag{3}$$

The locus of points satisfying equation (2), which always lies inside the chemical spinodal, is defined as the coherent spinodal and is shown in Figure 1(b).

These are some of the general concepts of spinodal decomposition.

For more detailed discussion, reviews written by Hilliard [7], Hoffman [15], Cahn [16], and Ditchek and Schwartz [2] are available.

1.2 Mechanical Properties in Spinodal Alloys

The first model of the age-hardening in spinodal alloys was proposed by Cahn [1]. He assumed that the composition fluctuations are best described as the sum of three prependicular cosine waves with directions along the cubic <100> type axes. He then discussed the force on a single dislocation due to the internal stresses developed by the composition fluctuation. The critical resolved shear stress (CRSS) was then defined by the maximum value of the applied stress under which the completely periodic shape of the dislocation is stable. To obtain the CRSS, Cahn approximately solved a force balance equation for an edge and a screw dislocation by considering the applied force, the coherency internal force and dislocation self force. The CRSS for a screw dislocation, for example, is obtained as [1]

$$\sigma_c = \frac{A^2 \eta^2 \lambda Y^2 b}{6\sqrt{6}\pi\gamma} \quad , \tag{4}$$

where λ is the wavelength, A is the amplitude of the composition modulation, b is the magnitude of the Burgers vector and γ is the self energy per unit length of the dislocation. From equation (4), it can be seen that Cahn's theory gives the increase in yield stress proportional to $A^2\lambda$. In the usual case of spinodal decomposition, it is experimentally known that $A\eta$ has an order of magnitude 10^{-2}, λ is approximately around 100 Å, b is 2 to 3 Å, $Y \simeq 10^{11}$ N/m^2 and $\gamma \simeq 10^{-8}$ N. Therefore, the typical value of the CRSS predicted by Cahn is around

5 MN/m^2.

Unfortunately, his prediction in the CRSS was proven to be too small. For example, according to the Capenter's study [17] of Au-Pt spinodal alloy, the observed yield strength (~70 MN/m^2) was much larger than Cahn's yield stress. Similar disagreement has also been found by Douglass and Barbee [18], Ditchek and Schwartz [2], and Lefevre et al. [19]. Moreover, the $A^2\lambda$ dependence of the incremental yield stress was also found to be unapplicable by Butler and Thomas [20] and Lefevre et al. [19]. In order to overcome the above mentioned disagreement between the Cahn's theory and the experimental data, several other theoretical models have been proposed.

Dahlgren obtained a theoretical expression of CRSS in FCC spinodal alloys as [21, 22]

$$\sigma = \frac{1}{3\sqrt{6}} A\eta Y \ . \qquad (5)$$

Equation (5) is derived by considering the coherency internal stress and its interaction with a glide dislocation.

Generally, his expression gives better agreement with experimental data [2]. In fact, by using the same representative values as before ($A\eta \simeq 0.01$, $Y \simeq 10^{11}$ N/m^2), equation (5) gives the CRSS ~140 MN/m^2 which is much larger than the one give by equation (4). However, in spite of this agreement with experimental data, Dahlgren's theory does not seem to be acceptable either. This is because he tacitly assumed the straight dislocation to obtain equation(5) which,as will be shown later, can not be justified in the existence of an internal stress field.

Carpenter [17] as well as Ditchek and Schwartz [23] proposed the

lattice mismatch theories. They considered the mismatch between a lower and an upper half of a slip plane due to the difference in the lattice parameter when a dislocation cuts through the modulated structure. Contrary to their discussion, we believe that the idea of the lattice mismatch is equivalent to the consideration of coherency stress if the continuum elastic theory is applied. Thus, their theories correspond to the consideration of the contribution of the coherency internal stress using the different approximation. Since they again neglected the important role of the dislocation self stress, their theories are not considered to be satisfactory.

Ghista and Nix [24] claimed that the elastic inhomogeneity, i.e., the spacial variation of the elastic modulus, in the modulated alloy is responsible for the age-hardening. Their theory suggests that the CRSS increases linearly with the amplitude of the shear modulus variation and inversely with the wavelength. However, their theory was also proven to be unrealistic [3]. Firstly, they only considered a straight dislocation and neglected the contribution by the internal coherency stress. Secondly, even when the Bessel function approximation of the radial variation of the shear modulus is permitted to appear in their theory [21], one can not rely on their calculation that the resultant self energy of the dislocation is also a damping function of the position. Since the elastic inhomogenity is distributed periodically in their model, the self energy should also be a completely periodic function of the position.

Ditchek and Schwartz [25] obtained an empirical equation of age-hardening, i.e., the incremental yield stress in spinodal alloys, as

$$\Delta YS = cA + dA \frac{\lambda-\lambda_o}{\lambda} , \qquad (6)$$

where c, d and λ_o are constants depending on the material itself. According to their recent experiment by using a Cu-10Ni-6Sn spinodal alloy [26], the amplitude A initially increases rapidly as the aging time increases while the wavelength λ remains almost constant during the early stage of decomposition. This indicates that if we accept equation (6), the age-hardening ΔYS, at least initially, is proportional to A. In fact, Butler and Thomas [20] in their experiment using Cu-Ni-Fe alloy also observed that the yield stress is proportional to A and independent of λ. According to equation (6), the contribution of wavelength λ on ΔYS should occur at the later stages of decomposition where λ begins to increase as the aging time becomes longer. However, at later stages, the modulation profile can no more be assumed as cosinusoidal. This is because at the very last stages of aging, equilibrium two-phase coexistence should be observed (as we discussed in the previous section) and the modulation wave in this case will be the "square wave" which can only be expressed in terms of Fourier series. Thus, the accurate experimental determination of A and λ using x-ray diffraction becomes very difficult. Because of this, it is still doubtful whether equation (6) is thoroughly applicable regardless of the stages of decomposition. Therefore, we would like to limit ourselves to the situation where the approximation of the cosinusoidal variation of the composition modulation is considered to be reasonable, i.e., the relatively earlier stages of the decomposition.

Most recently, Kato, Mori and Schwartz [3, 27] proposed a new

approach to understand the age-hardening. Their discussion is similar to Cahn's theory, i.e., based on the same force balanace equation as Cahn used. The difference is that they considered that a mixed dislocation, having the minimum energy configuration and the largest resistance from the internal stress field, was responsible for macroscopic yielding. Their results, predicting a much larger CRSS than Cahn's theory and the CRSS is proportional only to A', are in agreement with experiments [3, 27].

Since this theory (the K-M-S theory) is believed to be the most rigorous and the most reasonable explanation so far, a more detailed review of the K-M-S theory necessary for the present work will be shown later.

1.3 Temperature Dependence of Incremental Yield Stress in Spinodal Alloys

Lagneborg [5] measured the temperature dependence of the yield stress and the activation volume by evaluating the athermal stress and thermal stress during 475^{o}C aging of a spinodal Fe-Cr alloy. His results show that the hardening due to aging occurs mostly by an increase of the athermal stress (~80% of the total stress) and the incremental yield stress is almost temperature independent.

The temperature and strain-rate dependence of the yield and flow stresses and the activation volume during plastic deformation of a Cu-Ni-Sn spinodal alloy were also examined by Kato and Schwartz [6]. They found that the incremental yield stress of an aged alloy showed little temperature dependence. They also suggested that the internal stress barrier caused by spinodal decomposition is too large for a

glide dislocation to overcome thermally.

In spite of those experimental data, there has been no reasonable theoretical explanation as to why the incremental yield stress is essentially temperature and strain-rate independent. Lagneborg, in his paper [5], explained the above mentioned experimental data using William's theory [28], i.e., by considering the interaction between the hydrostatic stress field of an edge dislocation and a precipitate.

However, this explanation does not seem satisfactory [3]. First of all, the incremental yield stress in his result can only apply to the case when the volume fraction of the precipitate is small. Secondly, for the case of spinodal alloys, not only the edge component but also the screw component of a dislocation can interact with the internal stress. Thus, the problem still remains to be solved, i.e., "Why is the age-hardening in spinodal alloys temperature independent?" The main purpose of the present research is to answer this question by using an appropreate model applicable to spinodal alloys. Because of the reasons mentioned before, we will use the K-M-S theory and develop their idea by taking into account the thermally activated process of dislocation motion.

In the following chapters, the theories behind the present research will be discussed, and in chapter 4, the theory of thermally activated dislocation motion in spinodal alloys, developed in the present research, will be shown.

2 FORCES ACTING ON A DISLOCATION

From the Peach-Koehler equation, the force, $\vec{f} = (f_1, f_2, f_3)$, acting on the unit length of dislocation can be written as

$$f_m = - (\sigma^S_{ij} + \sigma^I_{ij} + \sigma^A_{ij})\varepsilon_{jmn} b_i \nu_n \quad , \qquad (7)$$

where σ^S_{ij} is the dislocation self stress, σ^I_{ij} is the internal stress, σ^A_{ij} is the external applied stress, ε_{jmn} is the permutation tensor as

$$\begin{cases} \varepsilon_{123} = \varepsilon_{231} = \varepsilon_{312} = 1 \\ \varepsilon_{132} = \varepsilon_{213} = \varepsilon_{321} = -1 \\ \text{others} \qquad\qquad = 0 \end{cases} ,$$

$\vec{b}$ (b_1, b_2, b_3) is the Burgers vector and $\vec{\nu}$ (ν_1, ν_2, ν_3) is the dislocation line vector of unit length. Here the usual summation convention of repeated indices is used.

In the present study, we consider a glide dislocation on a slip plane in which a two-dimensional periodic potential field is distributed. If the stationary shape of the dislocation is considered, the total force acting on the dislocation, f_m, should be zero. By defining

$$f_k = f^k_m = -\sigma^k_{ij} \varepsilon_{jmn} b_i \nu_n \quad ,$$

we can obtain the force-balance equation as

$$f_S + f_I + f_A = 0 . \qquad (8)$$

From this equation, one can find the stationary shape of the dislocation. In order to do that, let us first consider these three forces one by one for the case of spinodal alloys.

2.1 Internal Force Due to the Periodic Internal Stress Field

The internal stress field of a spinodal alloy is coming from its composition modulation. For the general case of an alloy with a cubic structure, one can usually assume that the composition modulation takes place along the three <100> directions. This is because in these directions, the elastic strain energy required to maintain coherency is minimum [7]. Thus, let us assume for simplicity this modulation to be a cosinusoidal function with amplitude 3A [13], that is,

$$C - C_o = A(\cos\beta x + \cos\beta y + \cos\beta z), \qquad (9)$$

where $\beta = 2\pi/\lambda$, λ is the wavelength of the three dimensional composition modulation; C and C_o are respectively the local and the average atomic concentrations of the secondary element and x, y and z axes are taken to be parallel to the three <100> directions.

If $\eta = \frac{1}{a}\partial a/\partial c$ describes the compositional variation of stress-free lattice parameter, a, the internal stress field σ^I_{ij} can be written as [1]

$$\sigma^I_{ij} = \begin{pmatrix} S_2(y)+S_3(z) & 0 & 0 \\ 0 & S_3(z)+S_1(x) & 0 \\ 0 & 0 & S_1(x)+S_2(y) \end{pmatrix}, \qquad (10)$$

with

$$S_1(x) = -A\eta Y\cos\beta x,$$
$$S_2(y) = -A\eta Y\cos\beta y,$$
$$S_3(z) = -A\eta Y\cos\beta z,$$

where Y has the same meaning as defined in chapter 1. In case of isotropic elasticity, Y reduces to [7]

$$Y = E/(1 - \nu),$$

where E is the Young's modulus and ν is the poisson's ratio. Using the Peach-Koehler equation as well as equation (10), the forces exerted on a dislocation by this internal stress field can be written as [1]

$$f_I = -(n_1 b_1 S_1 + n_2 b_2 S_2 + n_3 b_3 S_3) \ , \qquad (11)$$

where $\vec{n} = (n_1, n_2, n_3)$ is the unit normal vector to the slip plane. For FCC spinodal alloys, the slip plane (111) can be written as

$$x + y + z = \sqrt{3}d \ , \qquad (12)$$

where d is the interplaner distance between the (111) planes. The resolved force on a dislocation with the Burgers vector parallel to the $[1\bar{1}0]$ slip direction becomes from equation (11) as

$$f_I = \sqrt{\frac{2}{3}}A\eta Yb\sin\left[\sqrt{\frac{1}{2}}\beta(x + y)\right]\sin\left[\sqrt{\frac{1}{2}}\beta(x - y)\right] \ . \qquad (13)$$

Rotating the coordinate system such that the x is along the $[1\bar{1}0]$ and

y along the [11$\bar{2}$] and combing with equation (12) we have the force due to the internal stress field as [1]

$$f_I = \sqrt{\frac{2}{3}}\, A\eta Yb \sin\left(\frac{1}{\sqrt{6}}\beta y\right) \sin\left(\frac{1}{\sqrt{2}}\beta x\right). \qquad (14)$$

From the above equation, the (111) slip plane thus resembles a rectangular checkboard of alternating forces as shown in Figure 2. The sides of the rectangles are the locus of zero force positions, and within each rectangle the + or - sign represents the maximum or minimum force which has an extreme in the center.

2.2 Self Force Due to the Curvature of Dislocation

In the presence of the internal stress discussed in the previous section, the dislocation should be curved at equilibrium. If the radius of curvature of the dislocation line is ρ and the self energy of the dislocation per unit length is γ (γ can be roughly approximated as Gb^2 where G is the shear modulus), then the force acting on the unit length of dislocation due to this curvature can be written as

$$f_S = \frac{\gamma}{\rho}, \qquad (15)$$

Here, the line-tension approximation of dislocation is applied. The curvature of the dislocation k is defined as

$$k = \frac{1}{\rho} = \frac{\dfrac{d^2y}{dx^2}}{\left[1 + \left(\dfrac{dy}{dx}\right)^2\right]^{3/2}} \quad . \qquad (16)$$

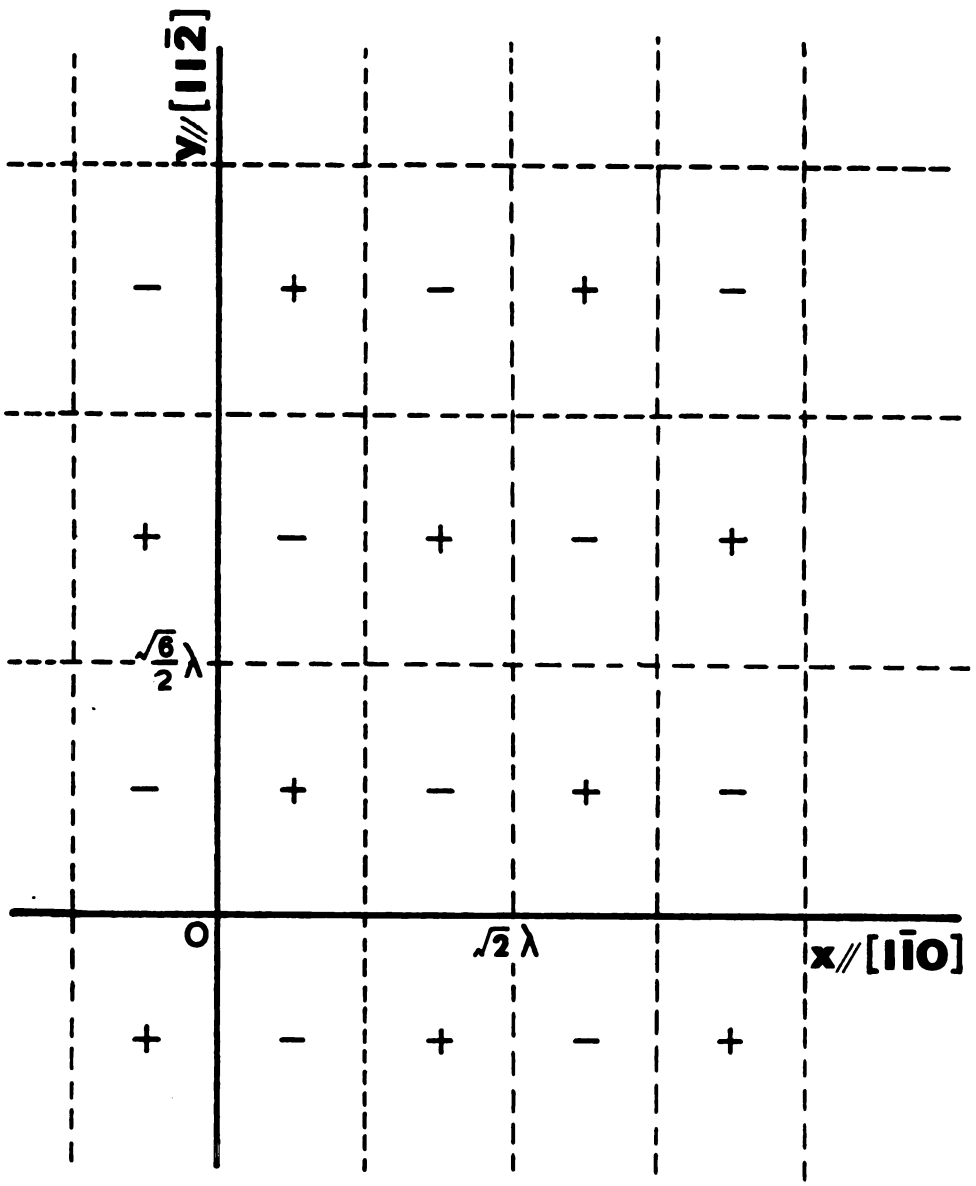

Figure 2 Schematic representation of the internal stress profile.

Substituting equation (16) into equation (15), we have the force due to the curvature of the dislocation as

$$f_S = \frac{\gamma\left(\frac{d^2y}{dx^2}\right)}{\left[1 + \left(\frac{dy}{dx}\right)^2\right]^{3/2}} \quad . \tag{17}$$

2.3 Force Due to the External Applied Stress

If the external resolved shear stress σ is applied, then the interaction force between the unit length of the dislocation and the applied stress can be written as

$$f_A = \sigma b \ . \tag{18}$$

2.4 The Force Balance Equation for an FCC Spinodal Alloy

According to the force balance equation mentioned before, when the dislocation is at a stationary configuration, the above three forces must satisfy equation (8). Therefore, for a dislocation in a spinodal modulated structure, we have

$$\frac{\gamma\left(\frac{d^2y}{dx^2}\right)}{\left[1 + \left(\frac{dy}{dx}\right)^2\right]^{3/2}} + \sqrt{\frac{2}{3}}\, A\eta\gamma b \sin\left(\frac{1}{\sqrt{2}}\beta x\right)\sin\left(\frac{1}{\sqrt{6}}\beta y\right) + \sigma b = 0. \tag{19}$$

This is the force balance equation for a dislocation on the (111) [1$\bar{1}$0] system in an FCC spinodal structure.

3 YIELDING BY A MIXED DISLOCATION:

Brief Review of Kato-Mori-Schwartz Theory

As mentioned briefly before, Kato, Mori, and Schwartz considered that the macroscopic yielding in FCC spinodal alloys is controlled by the motion of a mixed dislocation rather than an edge or screw dislocation discussed by Cahn [1]. This is because the free energy per unit length in the mixed dislocation is smaller than that in the edge or screw dislocation. This indicates that the configuration of the mixed dislocation is energetically more favorable. Since a dislocation tends to lie as much as possible in a position of lowest free energy, therefore, in the present case, the macroscopic yielding is determined by the motion of the mixed dislocation which has the minimum energy configuration and the largest resistance from the internal stress field.

To describe the mixed dislocation configuration, it is more convenient to introduce new variables u and v as [3]

$$u = \frac{x}{\sqrt{2}} - \frac{y}{\sqrt{6}} - \frac{\pi}{\beta} \quad .$$

$$v = \frac{x}{\sqrt{2}} + \frac{y}{\sqrt{6}} \quad . \tag{20}$$

By using the above transformation, as in Figure 3, we can rewrite equation (19) as

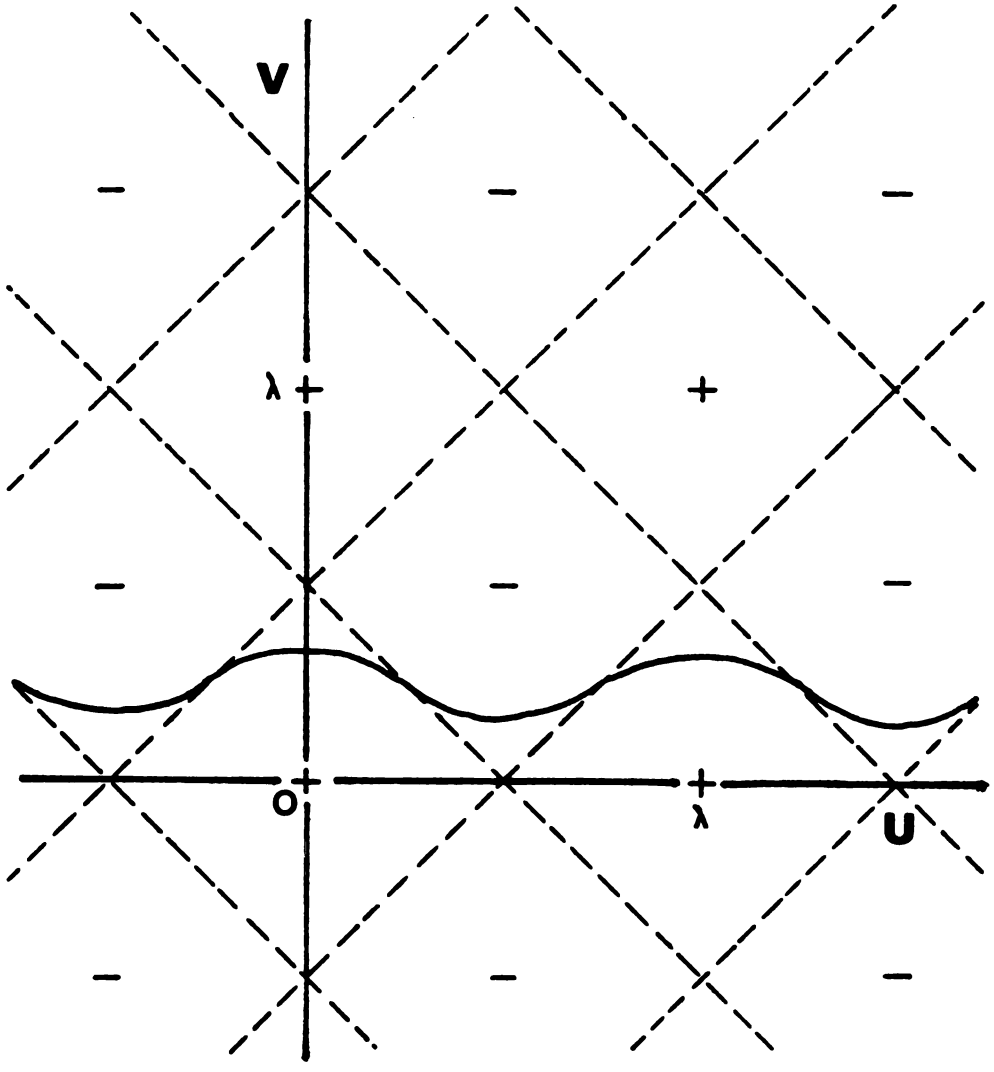

Figure 3 Rotating the coordinate axes of the internal stress profile, Figure 2.

$$\frac{\sqrt{6}}{4}\frac{\gamma\left(\frac{d^2v}{du^2}\right)}{\left[1+\left(\frac{dv}{du}\right)+\left(\frac{dv}{du}\right)^2\right]^{3/2}} + \frac{1}{\sqrt{6}}A\eta\gamma b(\cos\beta v + \cos\beta u) + \sigma b = 0. \quad (21)$$

Since equation (21) is a nonlinear differential equation, the Galerkin method is applied to approximately solve this equation analytically. To apply this method, we assume that $|\frac{dv}{du}|$ is much smaller than the unity (this assumption will be justified later). Therefore, the derivatives in the denominator of the first term in equation (21) can be neglected.

The stable shape of the dislocation is assumed to be cosinusoidal, i.e.,

$$v = C_1 + C_2 \cos\beta u \ , \quad (22)$$

where C_1 and C_2 are unknown parameters to be determined. Since $|\frac{dv}{du}|$ is much smaller than one, or equivalently βC_2 is much smaller than one, the following approximation can be used.

$$\cos\beta v \simeq \cos\beta C_1 - \beta C_2 \sin\beta C_1 \cos\beta u \ . \quad (27)$$

Adopting the Galerkin method together with equation (27), C_1 and C_2 are obtained as [3]

$$\cos\beta C_1 = -\sqrt{6}\sigma/A\eta\gamma \ ,$$

$$C_2 = \frac{6A\eta\gamma b\gamma\beta - 4A\eta\gamma b^2\sqrt{A^2\eta^2\gamma^2 + 6\sigma^2}}{(24\sigma^2b^2 + 9\gamma^2\beta^2 - 4A^2\eta^2\gamma^2b^2)\beta} \ . \quad (24)$$

From equation(24), if $|\sigma|$ is larger than $A\eta Y/\sqrt{6}$, no stable solution can exist. Therefore, the critical resolved shear stress (CRSS), σ_c, can be written as

$$|\sigma_c| = A\eta Y/\sqrt{6} \ . \qquad (25)$$

This value obtained by Kato, Mori and Schwartz corresponds to the incremental CRSS in the aged spinodal alloy [3]. In usual spinodal alloys, $A\eta Y/\gamma\beta$ is in the order of magnitude $\sim 10^{-2}$ [3, 6]. This means C_2 is much smaller than λ (wavelength) from equation (24). Thus, the original assumption that $|\frac{dv}{du}|$ is much smaller than unity is justified. In fact, it has been demonstrated [3] that the numerical solution of equation (21) by a computer gives essentially the same value of the CRSS as equation (25).

Now, let us evaluate equations (24) and (25) by using experimental values. From a 623 K, 20 minutes aged Cu-10Ni-6Sn alloy [3], i.e., $\gamma = 5.0 \times 10^{-9}$ N, $A = 1.6 \times 10^{-2}$, $\eta = 0.25$, $Y = 11.5 \times 10^{10}$ N/m^2, $b = 2.57 \times 10^{-10}$ m and $\lambda = 5.0 \times 10^{-9}$ m, we can obtain C_1 and C_2 and the stable shape of the dislocation. From equation (25), the incremental CRSS is calculated as 187 MN/m^2 in good agreement with experimental data [3]. This is the outline of the K-M-S theory upon which the present research is based. In the next chapters, the K-M-S theory will be expanded and applied to discuss the thermally activated process of deformation in spinodal alloys.

4 THERMALLY ACTIVATED DOUBLE-KINK FORMATION IN A DISLOCATION IN A SPINODAL ALLOY

So far we have not taken into account the thermally activated process of the dislocation motion. Thus, equation (25) actually corresponds to the CRSS at 0 K [3]. In other words, the solutions (24) are for the stable shape of the dislocation. In order to discuss the thermally activated process of the dislocation motion, we must calculate the saddle-point (unstable) configuration of the mixed dislocation in addition to the stable configuration as a function of the applied stress from equation (21)*. Since equation (21) is a non-linear differential equation, it is difficult to obtain this unstable shape analytically. Thus, numerical calculation by using a computer was applied for this problem.

It should be noted that a single thermal activation event occurs locally and, thus, it is reasonable to assume that $v_u(u)$ approaches to $v_s(u)$ if u is far away from the position where the activation event is taking place. Here, the subscript "u" and "s" represent "unstable" and "stable" respectively. In other words, we are dealing with the situation where both ends of the unstable dislocation line approached asymptotically to the stable dislocation configuration. Therefore,

---

* As will be shown later, equation (21) actually gives all stationary shapes of the dislocation. Thus, the saddle-point configuration can also be obtained from equation (21) by choosing the appropreate initial conditions.

with this in mined, the initial conditions, $v_u(0)$ and $dv_u(0)/du$, to calculate the unstable dislocation configuration of mixed character as a function of the applied stress from equation (21) can be chosen.

Judging from the internal stress profile (Figure 3), let us first fix one of the initial conditions as

$$\frac{dv_u}{du} = 0 \quad \text{at } u = 0 \ . \tag{26}$$

The other initial condition, i.e., the value of $v_u(0)$, is not yet clear at this moment. Figure 4 schematically shows the results of the numerical calculation to obtain the unstable dislocation shapes from equation (21) by choosing three different values of $v_u(0)$ as well as equation (26). As for curve (a), since the initial value $v_u(0)$ was set too small, the dislocation did not go back to its stable positions, right-hand side of the dislocation having smaller values of v than the left-hand side. For curve (c), the opposite situation occurs, the dislocation goes too high after the double-kink is formed. Both of these situations are contradictory to the requirement mentioned in the previous paragraph. Only if we adjust $v_u(0)$ to a specific value, as in curve (b), we can obtain the double-kink shape of the dislocation which we were looking for. This is called the "shooting method".

Interestingly, we found that the values of the right initial conditions for curve (b) are almost the same as those used to obtain the approximate shape of the stable dislocation, i.e.,

$$\begin{cases} v_u(0) = C_1 + C_2 \\ \dfrac{dv_u}{du} = 0 \end{cases} \quad \text{at } u = 0 \ . \tag{27}$$

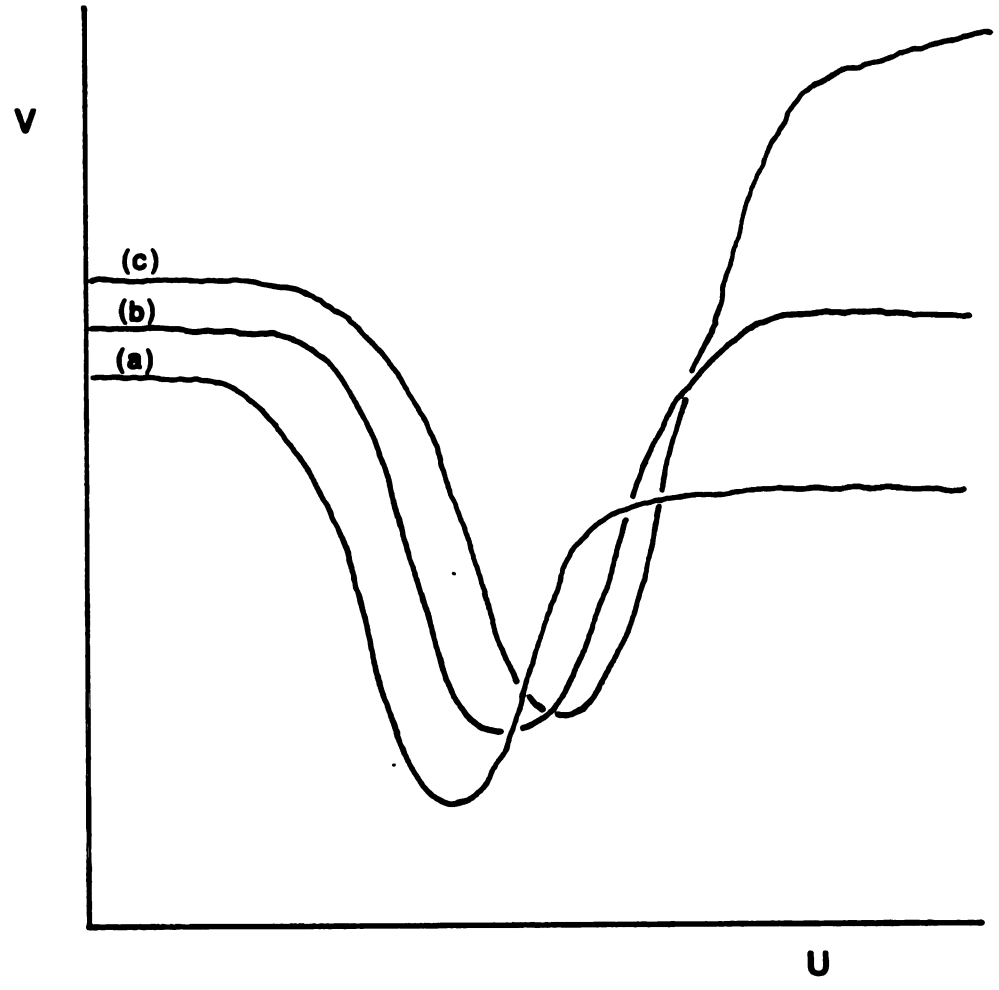

Figure 4 Schematic representation of the "shooting method".

We think that this seemingly strange coicidence is due to the following reasons. Since equation (24) are just approximate solutions (although practically accurate enough), equation (26) are very slightly different from the exact values for the completely periodic stable dislocation; therefore, as the numerical integration of equation (21) proceeds from $u = 0$ to $u > 0$, the deviation from the stable shape dislocation becomes larger and larger, and eventually the formation of the double-kink is attained.

Therefore, we can select the initial conditions from those for the stable shape dislocation and obtain the required result. By repeating the above numerical calculation, we can obtain the double-kink configuration of the dislocation for different values of the applied stress as shown in Figure 5. The relative positions of the double-kinks arearranged along the u-direction so that the comparison becomes easier. In the absence of the applied stress, one single kink is formed. When the applied stress is larger than zero, the following results can be observed.

(1) The shape of the double-kink is similar to that in the one-dimensional internal stress field [29].

(2) The height of the double-kink is a decreasing function of the applied stress.

(3) The width of the double-kink is an increasing function of the applied stress.

We will discuss these characteristics in the later chapters.

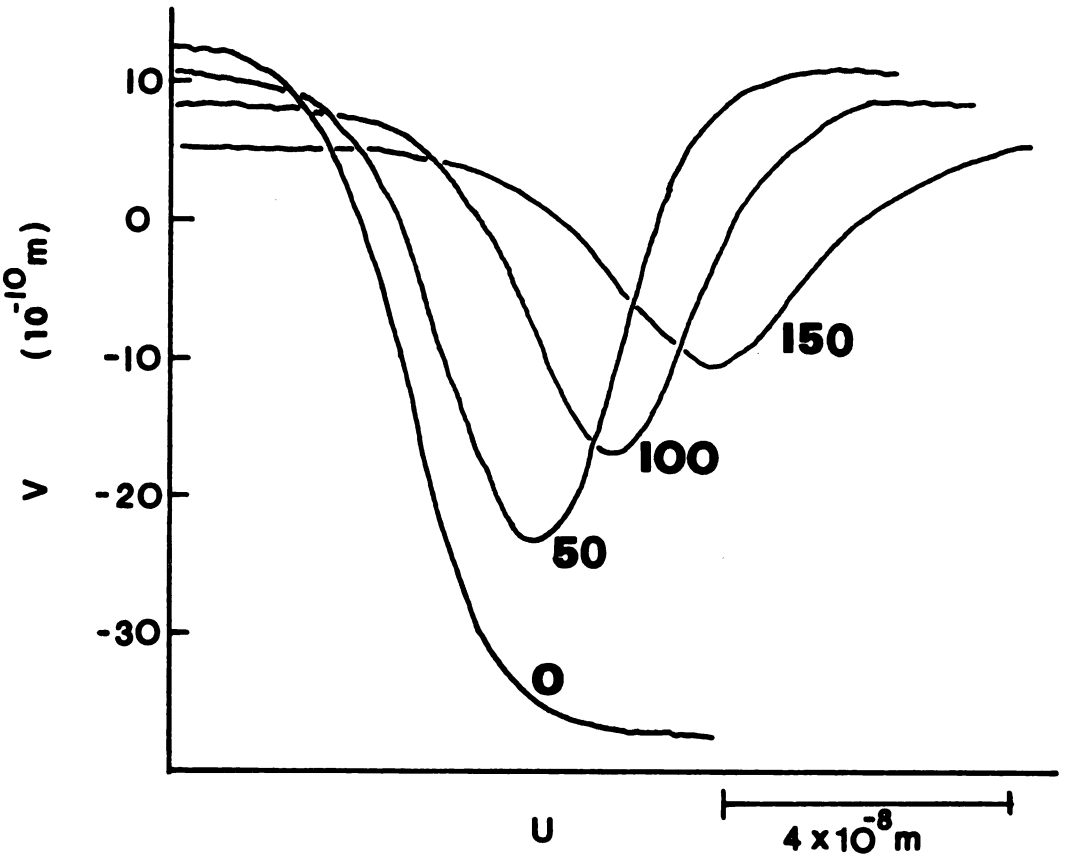

Figure 5 Saddle-point configuration of the dislocation for different values of the external applied stress.

5 CALCULATION OF ACTIVATION ENERGY AND ACTIVATION VOLUME

5.1 Activation Energy

The activation energy is defined as the energy necessary to activate a dislocation from its stable position to its unstable (saddle-point) poistion or the free energy difference between the stable and the unstable dislocations.

The total free energy of a dislocation having a shape $y = y(x)$ can be described as [3]

$$F = \int_{-\infty}^{\infty} \left\{ \gamma \sqrt{1 + \left(\frac{dy}{dx}\right)^2} + V(x, y) - \sigma b y \right\} dx \quad , \tag{28}$$

where the first term in equation (28) is the self energy of the dislocation due to its curvature, the second term is the interaction energy between the internal stress and the dislocation, and the third term is the work done by the external shear stress σ to move this dislocation. The stationary value of F can be obtained by taking the eulerian equation of equation (28), i.e., the stationary shape of the dislocation must satisfy

$$\frac{\gamma \left(\frac{d^2y}{dx^2}\right)}{\left[1 + \left(\frac{dy}{dx}\right)^2\right]^{3/2}} - \frac{\partial V}{\partial y} + \sigma b = 0 \ . \tag{29}$$

This is actually the rigorous derivation of the force balance equation

we discussed in chapter 2. It should also be noted that equation (29) gives not only stable (lowest energy) configuration of the dislocation but also all possible stationary (metastable and locally stable) configurations.

If we use the u-v coordinate system defined earlier, equation (29) becomes equation (21). From equation (21), we can obtain

$$V(u, v) = -\frac{1}{2} A\eta\gamma b \left\{ \frac{1}{\beta} \sin\beta v + v\cos\beta u \right\} , \qquad (30)$$

and equation (28) can be rewritten as

$$F = \sqrt{2} \int_{-\infty}^{\infty} \left\{ \gamma_N \sqrt{1+\left(\frac{dv}{du}\right)+\left(\frac{dv}{du}\right)^2} - \frac{1}{2} A\eta\gamma b \left(\frac{1}{\beta} \sin\beta v + v\cos\beta u \right) - \frac{\sqrt{6}}{2} \sigma b v \right\} du. \qquad (31)$$

Since the activation energy is defined as the free energy difference between the stable and the unstable shape dislocation, it can now be written as

$$F^* = \sqrt{2} \int_{-\infty}^{\infty} \left\{ \gamma_N \sqrt{1+\left(\frac{dv_u}{du}\right)+\left(\frac{dv_u}{du}\right)^2} - \gamma_N \sqrt{1+\left(\frac{dv_s}{du}\right)+\left(\frac{dv_s}{du}\right)^2} \right.$$

$$- \frac{1}{2} A\eta\gamma b \left[\frac{1}{\beta} (\sin\beta v_u - \sin\beta v_s) + (v_u - v_s)\cos\beta u \right]$$

$$\left. - \frac{\sqrt{6}}{2} \sigma b (v_u - v_s) \right\} du \quad . \qquad (32)$$

Since we have already obtained $v_u(u)$ and $v_s(u)$ in the previous section, we can carry out the numerical integration in equation (32) to obtain

the activation energy F*. Figure 6 shows the calculated results of F* as a function of the applied stress using the same numerical values as used in chapter 3 (P. 20). It can be seen in Figure 6 that F* decreases as the applied stress increases. The magnitude of the F* and its dependence on the applied stress will be discussed in the next chapter.

5.2 Activation Volume

The activation volume is defined as the area swept by the dislocation times its Burgers vector or the partial derivative of activation energy with respect to applied stress. It can be written as

$$v^* = -\frac{\partial F^*}{\partial \sigma} = \sqrt{3}b\int_{-\infty}^{\infty}(y_s - y_u)\,du \quad . \tag{33}$$

Figure 7 shows the calculated results of v* as a function of applied stress by a computer. In the case of zero applied stress, v* was estimated conventionally by calculating twice of the area with the single kink.

It should be noted that although the general tendency of the dependence of the activation volume v* on the applied stress is quite similar to that observed in the Peierls mechanism [30, 31], the present calculation gives much larger values of the activation volume. This will be discussed later.

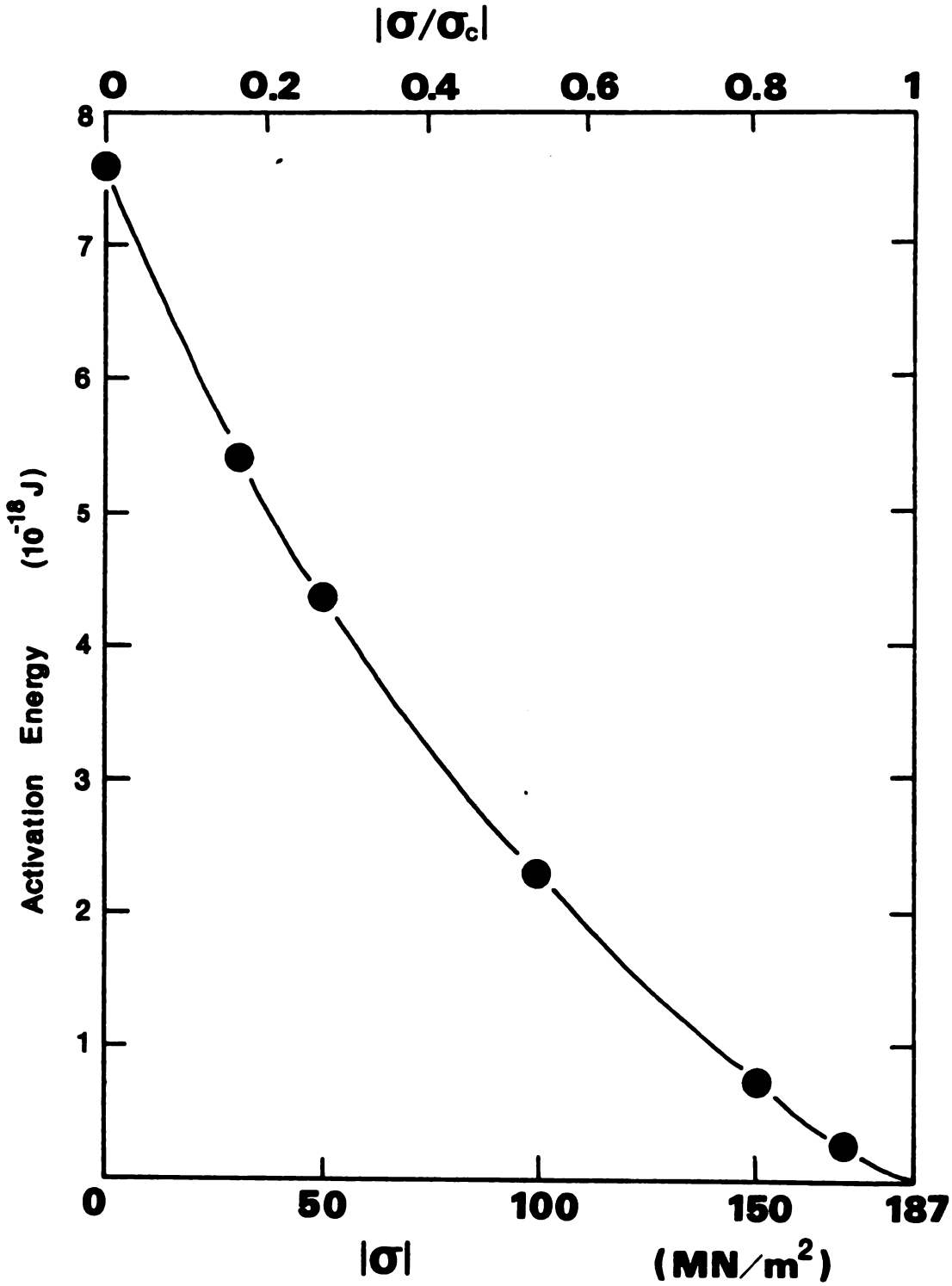

Figure 6 Activation energy vs. external applied stress curve.

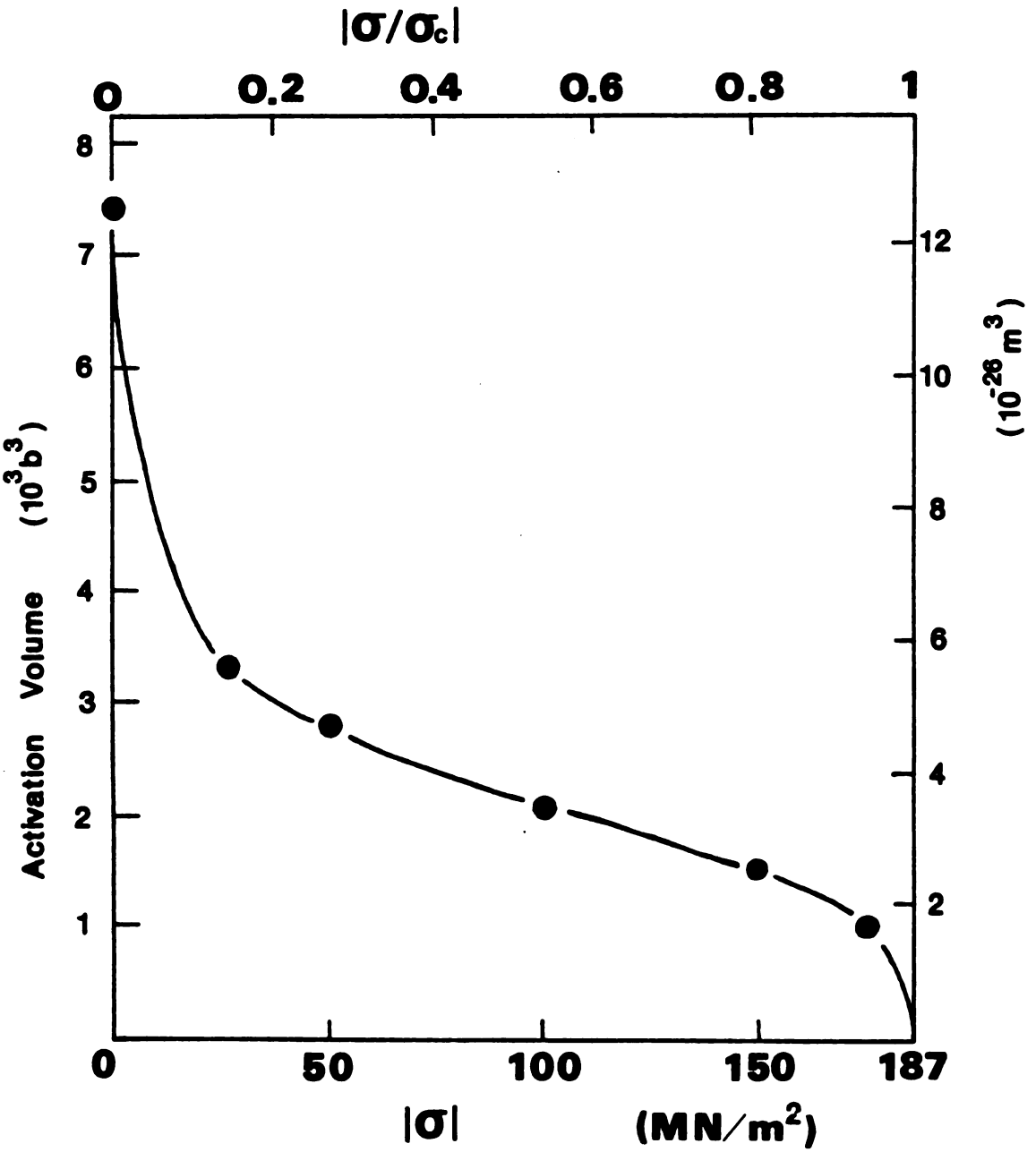

Figure 7 Activation volume vs. external applied stress curve.

6 DISCUSSION

6.1 Thermally Activated Dislocation Motion in Spinodal Alloys

As has been mentioned earlier, Kato and Schwartz [6] experimentally have found the temperature independence of age-hardening in an FCC Cu-10Ni-6Sn spinodal alloy. Similar results have also been observed by Lagneborg for BCC Fe-Cr spinodal alloys [5]. From the results of our calculation of activation energy, we can now discuss these experimental phenomena from theoretical points of view.

Let us first consider the possibility of the thermally activated dislocation motion in spinodal alloys. According to Kuramoto et al. [32], yielding usually occurs when $F^* \sim 26$ kT, where k is the Boltzmann constant and T is the temperature. Around room temperatures, this gives the value of $\sim 10^{-19}$ J. In our calculation of activation energy, on the other hand, the value of F* in Figure 6 are much larger than 10^{-19} J unless the applied stress becomes very close to 187 MN/m^2. This means that the activation process does not occur until $|\sigma/\sigma_c|$ reaches very close to one (0.96) or the thermal energy has little effect on yielding even at room temperature. From the above discussion, we can conclude that the hardening due to the composition modulation in spinodal alloys should be essentially temperature independent.

6.2 Comparison with the Peierls Field

Let us compare the present results of F* with those for the Peierls yielding. If the applied stress is absent, F* can be

interpreted as the formation energy of a double-kink, E_f. For the case of the Peierls yielding in BCC metals, it is known that the E_f is in the magnitude around 10^{-19} J [30, 13], whereas in the present case (Figure 6), E_f amounts to 7.6×10^{-18} J. Therefore, the magnitude of the formation energy of the double-kink in the present study is about a factor of one hundred larger than that in the Peierls field. This large difference comes from the periodicity of the stress fields. In the Peierls field, the wavelength of the periodicity is about the length of Burgers vector ($\sim 2 \times 10^{-10}$ m), whereas in the present case, it is in the order of magnitude of the wavelength of modulation ($\sim 5 \times 10^{-9}$ m). This large difference also appears in the magnitude of the acitvation volume. In Figure 7, the calculated value of the activation volume is about $7.4 \times 10^3 b^3$ at zero applied stress which is much larger than the corresponding value ($\sim 50b^3$) in the Peierls field of BCC metals. Thus, we can also discuss from the viewpoint of the activation volume that such a giant double-kink formation should require much larger energy than the thermal energy. This is also the reason why age-hardening of spinodal alloy is temperature independent.

6.3 Comparison with One-dimensional Thermal Activation Process

The present study can be interpreted as a study of the thermally activated dislocation motion in a two-dimensional field and it can be compared with that in a one-dimensional field. Recently, Mori and Kato [29] developed the asymptotic form of activation energy for double-kink formation in a dislocation in a one-dimensional periodic field when the applied stress approaches to the maximum internal stress. They concluded that:

(a) Although the activation volume is a decreasing function of the applied stress, the width of the double-kink is an increasing function.

(b) The asymptotic form of the activation energy is proportional to $(1 - \bar{\sigma})^{1.25}$ where $\bar{\sigma}$ is the applied stress devided by the maximum internal stress.

In their study, excellent agreement was found between the conclusion (b) and the low temperature deformation data of BCC metals. This agreement in turn supports the validity of the conclusion (a). In the present study of two-dimensional case as mentioned in chapter 4, the conclusion (a) is true. It is important to emphasize that although the width of the double-kink increases as the applied stress becomes larger, the height of the double-kink, on the other hand, decreases faster and, as a result, the area swept by the double-kink (activation area) decrease. Secondly, the conclusion (b) can be examined from Figure 5. According to the computer calculation, the dependence of the activation energy on the applied stress shown in Figure 5 can be approximated in the range $0.85 < |\sigma/\sigma_c| < 1$ as

$$F^* = 5.18 \times 10^{-18} (1 - \sigma/\sigma_c)^{1.21} \text{ J} .$$

Here, the exponent 1.21 is again very close to 1.25 in the conclusion (b).

This agreement gives us an interesting possibility, i.e., the thermally activated double-kink formation might be universally understood by a unified theory regardless of the dimensionality of the internal stress profile. Before concluding this chapter, it should be

emphasized that until one year ago, people have believed that F* is proportional to $(1 - |\sigma/\sigma_c|)^2$ [33] rather than $(1 - |\sigma/\sigma_c|)^{1.25}$. Thus, the more detailed research along this line could most probably give us an important breakthrough in the understanding of the thermally activated process of deformation.

7 SUMMARY

1. The thermally activated motion of a glide dislocation in a spinodal modulated structure is discussed energetically.
2. It is found that a double-kink similar to that in a Peierls potential field can be formed in a two-dimensional periodic field caused by the composition modulation.
3. The values for the activation volume and the activation energy associated with the double-knik formation in a spinodal alloy are much larger than those in the Peierls field.
4. The present results are in good agreement with the experimental observations of the temperature and the strain-rate independence of the age-hardening pnenomonon in spinodally modulated alloys.
5. The asymptotic form of the activation energy and the shape of the double-kink are quite similar between one-dimensional and two-dimensional internal stress fields.

REFERENCES

1. Cahn, J. W., "Hardening by spinodal decomposition", Acta Metallurgica, 11, 1275 (1963).

2. Ditcheck, B. and Schwartz, L.H., Annual Review of Materials Science, 9, 219 (1979).

3. Kato, M., Mori, T. and Schwartz, L. H., "Hardening by spinodal modulated structure", Acta Metallurgica, 28, 285 (1980).

4. Kato, M., "Hardening by spinodally modulated structure in bcc alloys", Acta Metallurgica, 29, 79 (1981).

5. Lagneborg, R., "Deformation in an Iron-30% Chromium alloy aged at 475°C", Acta Metallurgica, 15, 1737 (1967).

6. Kato, M. and Schwartz, L. H., "The temperature dependence of yield stress and work hardening in spinodally decomposed Cu-10Ni-6Sn alloy", Materials Science and Engineering, 41, 137 (1979).

7. Hilliard, J. E., Phase Transformation, American Society for Metals, Ohio, 1970.

8. Daniel, V. and Lipson, H., Proceeding of Royal Society (London), Serial A, 181, 368 (1943).

9. Daniel, V. and Lipson, H., Proceeding of Royal Society (London), Serial A, 182, 378 (1944).

10. Hillert, M., "A solid-solution model for inhomogeneous system", Acta Metallurgica, 9, 525 (1961).

11. Hillert, M., D. Sc. Thesis, Massachusetts Institute of Technology, MA., (1956).

12. Hillert, M., Cohen, M. and Averbach, B. L., "Formation of modulated structures in Copper-Nickel-Iron alloys", Acta Metallurgica, 9, 536 (1961).

13. Cahn, J. W., "On spinodal decomposition", Acta Metallurgica, 9, 795 (1961).

14. Cahn, J. W., "On spinodal decomposition in cubic crystals", Acta Metallurgica, 10, 179 (1962).

REFERENCES

15. Hoffman, D. W., "The effect of atomic misfit on the coexistence and spinodal transformation boundaries in binary alloys", Acta Metallurgica, 26, 933 (1978).

16. Cahn, J. W., "Spinodal decomposition", Trans. AIME, 242, 166 (1968).

17. Carpenter, R. W., "Deformation and fracture of Gold-Platinum polycrystals strengthened by spinodal decomposition", Acta Metallurgica, 15, 1297 (1967).

18. Douglass, D. L. and Barbee, T. W., "Spinodal Decomposition in Al/Zn alloys", J. of Materials Science, 4, 121 (1969).

19. Lefevre, B. G., D'Annessa, A. T. and Kalish, D., "Age hardening in Cu-15Ni-8Sn alloy", Metallurgical Transactions, 9A, 577 (1978).

20. Butler, E. P. and Thomas, G. "Structure and properties of spinodally decomposed Cu-Ni-Fe alloys", Acta Metallurgica, 18, 347 (1970).

21. Dahlgren, S. D., Ph. D. Thesis, University of California,Berkley, CA. (1966).

22. Dahlgren, S. D., "Dislocation Interactions with internal coherency stresses in age-hardened Cu-Ni-Fe alloys", Metallurgical Transactions, 7A, 1661 (1976).

23. Ditchek, B. and Schwartz, L. H., Proceeding of the 4th International Conference on Strength of Metals and Alloys, 3, 1319 (1976).

24. Ghista, D. N. and Nix, W. D., "A dislocation model pertaining to the strength of elastically inhomogeneous materials", Materials Science and Engineering, 3, 293 (1968/69).

25. Ditchek, B., Ph. D. Thesis, Northwestern University, IL. (1977).

26. Ditchek, B. and Schwartz, L. H., "Diffraction study of spinodal decomposition in Cu- 10Ni-6Sn", Acta Metallurgica, 28, 807 (1980).

27. Kato, M., Mori, T. and Schwartz, L. H., "The energetics of dislocation motion in spinodally modulated structures", Materials Science and Engineering, 51, 25 (1981).

28. Williams, R. O., "Theory of precipitation hardening: isotropically strained system", Acta Metallurgica, 5, 385 (1957).

29. Mori, T. and Kato, M., "Asymptotic form of activation energy for double-kink formation in a dislocation in a one-dimensional periodic field", Philosophical Magazine A, 43, 1315 (1981).

REFERENCES

30. Dorn, J. E. and Rajnak, S., "Nucleation of kink pairs and Peierls' mechanism of plastic deformation", Transactions AIME, 230, 1052 (1964).

31. Arsenault, R. J., "The double-kink model for low temperature deformation of B.C.C.metals and solid solutions", Acta Metallurgica, 15, 501 (1967).

32. Kuramoto, E., Aono, Y. and Kitajima, K., "Thermally activated slip deformation between 0.7 and 77 K in high-purity Iron single crystals", Philosophical Magzine A, 39, 717 (1979).

33. Celli, V., Kabler, M., Ninomiya, T. and Thomson, R., Physical Review, 131, 58.